Research on Optimization of Onboard Magnetic Diagnostics System of Hall Thruster Plasma

IEPC-2005-140

Presented at the 29th International Electric Propulsion Conference, Princeton University, October 31 – November 4, 2005

Binyamin Rubin*
Faculty of Aerospace Engineering, Technion, I.I.T., Haifa, 32000, Israel

Alexander Kapulkin† and Moshe Guelman‡
Asher Space Research Institute Technion, I.I.T., Haifa, 32000, Israel

The paper is devoted to the development of Hall thruster plasma non-contact magnetic diagnostics methods applicable for onboard diagnostics system. The approach to Hall current structure determination using steady-state magnetic measurements proposed in our previous work is further developed. The approach is based on inverse magnetostatic problem solution using two-dimensional constrained regularization. Optimal number and positions of magnetic sensors were determined and the solutions using simulated measurements with and without simulated noise were obtained.

Nomenclature

B	=	magnetic flux density
e	=	unit positive electric charge
E	=	electric field
J	=	current density
n	=	electron number density
λ	=	regularization parameter

I. Introduction

MANY modern electric propulsion systems and in particular, Hall thrusters, are equipped with diagnostic packages. The main purpose of these packages is usually to investigate the thruster performance as well as the environment created during the electric propulsion systems operation and its influence on the spacecraft. The diagnostics of the internal thruster processes are also of great interest. The results of onboard measurements show that the operation of Hall thruster in space may differ from the operation during ground tests[1]. In order to understand the reasons of this difference the studies of processes in thruster acceleration channel should be done during flight. Another important reason for the creation of onboard diagnostics system is that it may provide the clues to understanding the possible thruster malfunctions. The obvious requirements to such systems are compactness, lightweight and capability of non-contact real-time measurements without affecting thruster operation.

* Ph.D. student, Faculty of Aerospace Engineering rubin@aerodyne.technion.ac.il.
† Senior Scientist, kapulkin@tx.technion.ac.il.
‡ Institute Director and Professor, Faculty of Aerospace Engineering, aerglmn@aerodyne.technion.ac.il.

In our previous works different types of onboard diagnostics systems capable of providing information on the internal processes in Hall thruster were proposed[2,3]. In this paper we continue the effort to develop the approach to creation of non-contact diagnostics system and interpretation of its measurements.

The paper is dedicated to the method of non-contact determination of the Hall current structure using magnetic field sensors. The structure of the Hall current was previously investigated using probe measurements[4] and using the method which requires the thruster switch-off during each measurements run[5-8]. The approach described in the present work allows to carry out the steady-state measurements, which is especially important for onboard system. In our previous work[3] we considered one-dimensional current distribution, in present work two-dimensional axisymmetric distribution of the Hall current density is considered.

II. Hall Current diagnostics

A. Direct problem

1. The method of solution

Direct problem is the calculation of the magnetic field (self-field) generated by the current. The algorithm of the direct problem solution is necessary to solve the inverse problem. Besides, the distribution of magnetic field was analyzed in order to determine optimal locations of the magnetic sensors. The magnetic field distribution in the Hall thruster is not exactly axially symmetric because of the outer magnetic coils. In most cases the deviation of the magnetic field distribution from axially symmetric may be neglected but in our case in order to measure the small field generated by the Hall current we should take it into account. Also, the outer magnetic screen in our case is not axisymmetric because of modification described below; therefore it is impossible to use simplified two-dimensional axisymmetric model and necessary to perform 3D calculations. The calculations were performed using one of the most commonly used engineering finite-element method (FEM) solvers ANSYS.

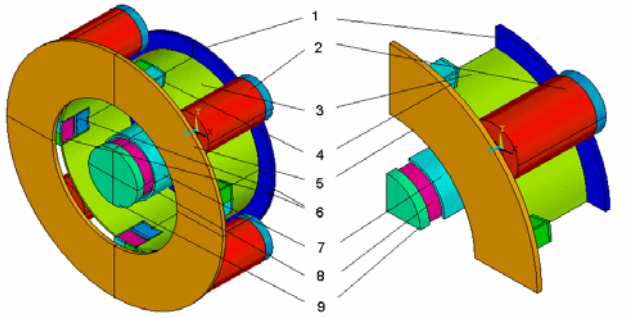

Figure 1. Full and ¼ sector model geometry of modified magnetic system.
1 – Backplane, 2 - outer magnetic coil, 3 - outer magnetic screen, 4 - modified part of the magnetic screen, 5 – outer magnetic pole piece, 6 – magnetic sensors, 7 - inner magnetic screen, 8 – inner magnetic coil, 9 - inner magnetic pole piece.

The model of magnetic system typical for present-day low-power Hall thruster was chosen for calculations. The cylindrical magnetic screen was modified near the thruster exit plane as described in Ref. 3. The modification allows to place the magnetic sensor in the vicinity of the Hall current. The measurements of the steady-state magnetic field can be carried out using commercially available magnetic sensors, such as Honeywell HTMC1021D sensor; the dimensions of the modified region were determined based on those of this sensor. The magnetic system used for calculations is shown in Fig. 1.

The Hall current distribution was approximated by cylindrical current elements, we determined that the size of each element 1.4 mm by 1.5 gives the sufficiently accurate results at reasonable computational time; the total number of elements was 130. It should be noted that while the problem is three-dimensional, the current distribution is axisymmetric and therefore it is treated as two-dimensional.

The solution of the inverse problem is an iterative process which includes one or more calculations of the direct problem solution at every iteration. It is possible to use the FEM solver in these calculations but the computational time in this case will be unreasonably high. Since the dependence between the current and the magnetic flux density may be considered as linear in the range of magnetic field values generated by the Hall current, the distribution of magnetic field may be obtained as the linear combination of the magnetic fields of individual elements. Calculating the magnetic field distribution generated by each of N current elements placing M magnetic field sensors each measuring one magnetic field component we obtain the linear matrix equation presented on Fig.2.

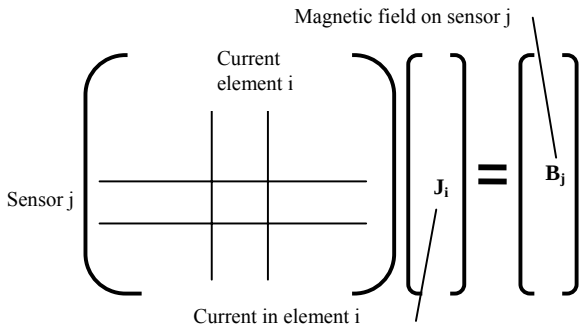

Figure 2. Linear system used for magnetic field calculation

The elements of this matrix are the values of magnetic field in different sensor locations generated by the current element carrying unit current. In order to calculate the magnetic field generated by certain current distribution this matrix is multiplied by the columnwise stacked vector of current distribution.

The obtained matrix may be easily checked in experiment using the method described in the Ref. 5-8. A metal coil carrying current should be placed into the acceleration channel and the magnetic field generated by the coil should be measured for different coil locations.

2. Results of the direct problem solution.

The radial magnetic field profiles for original and modified magnetic systems are presented on Fig. 3. The profiles closely match; the maximum difference of the centerline values is about 5 %.

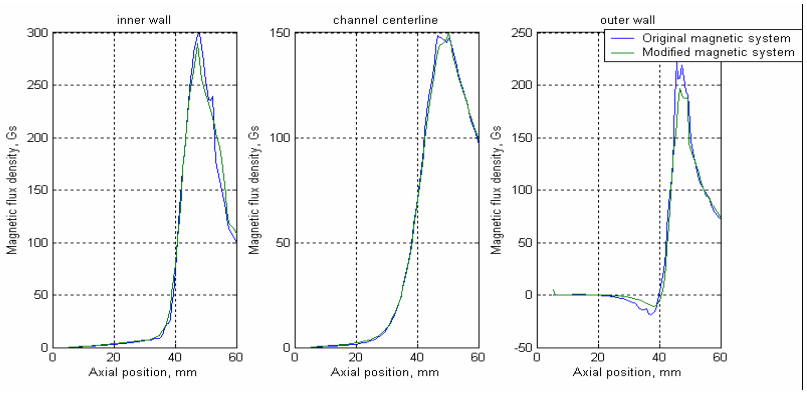

Figure 3. Comparison of radial magnetic field components in original and modified magnetic systems.

According to the different experimental data available up to date[4-8], Hall current is 3.5-15 times higher then the discharge current. For the Hall thruster model with dimensions used in our analysis discharge current value is about 2 A, therefore the Hall current value of 10 A was chosen as a conservative estimation.

For the purpose of simulating the magnetic field measurements the Hall current distribution was simulated using the Gauss distribution in radial direction and the following distribution in axial direction:

$$y = \frac{1}{\left(\frac{\sinh(a(x-c))}{\sinh(aq)}\right)^2 + 1} \tag{1}$$

This function includes three parameters, *a, c* and *q.* Parameter c determines the median of the distribution, parameter q determines the width of the distribution and parameter *a* determines the steepness of the slopes, x is the coordinate. This function was used for following reasons. The experimental data[4,8] show that the Hall current distribution has single maximum. In Ref. 8 the Gaussian distribution in radial and axial directions was used. However the results of calculations of plasma parameters distributions in Ref. 3 show that the axial distribution may be close to bell-shaped but more broad. This distribution allows obtaining both Gauss-like bell-shaped distributions and more wide distributions.

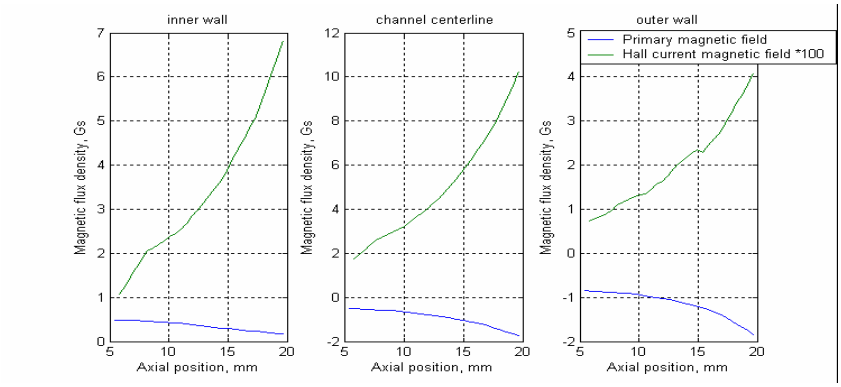

Figure 4. Axial magnetic field component distribution of the primary magnetic field and the Hall current self-field in the region close to the backplane.

In our calculations we have used the distribution of the Hall current density with the profile close to the experimentally measured[4] and a value of 10 A. The comparison of the primary magnetic field distribution with the distribution of the self-field generated by the Hall current in the region close to the backplane (behind the anode) where the magnetic sensors could be placed are presented on Fig. 4. To plot the distributions on the same scale the Hall current field was multiplied by the factor of 100. The magnitude of Hall current self-field makes several percent of the primary field and therefore may be measured by the existing magnetic sensors.

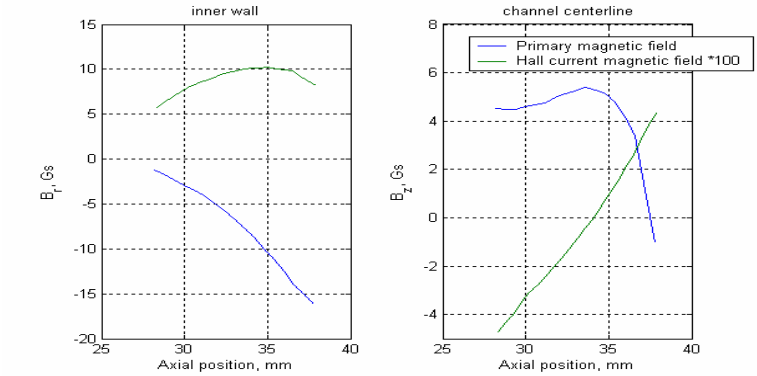

Figure 5. The comparison of the primary magnetic field and Hall current magnetic field in the region where the sensors may be placed.

The calculations proved that the magnetic measurements in that area do not provide the sufficient data for the determination of the Hall current distribution and therefore, as mentioned above, the modification of the magnetic screen described above should be made. The distributions of the radial and axial magnetic field components in the modified part of the magnetic system where the magnetic sensors could be placed are presented at Fig. 5.

The ratio of the self-magnetic field to the primary field in this region makes up to several percent and even more than that in the region where the axial component of the primary magnetic field is close to zero. Therefore it is possible to measure the self-magnetic field in this region.

B. Inverse problem.

The inverse problem in our case is the problem of determination of the current distribution from the measured magnetic field values. Since steady-state (time-averaged) current and magnetic field distributions are considered, the problem is an magnetostatic problem.

Solution of inverse magnetostatic problems has been discussed in the context of diagnostics of superconducting magnets[9], biomagnetism[10], identification of the plasma magnetic contour in the thermonuclear fusion area[11], determination of the ferromagnetic thin shell magnetization[12]. Different regularization methods were used in mentioned works: Truncated Singular Value Decomposition[11], iterative regularization[9], Levenberg-Marquard algorithm with regularization term[13]. In Ref. 12 instead of regularization the authors use the injection of the physical information to constrain the solution. In this work different method is presented based on Tikhonov regularization[14].

1. Inverse problem formulation.

As mentioned above, the axisymmetric distribution of azimuthal current density is parameterized using piecewise constant elements. The discretization of the problem leads to the following linear matrix equation for determination of the magnetic field distribution

$$A\boldsymbol{J}=B, \tag{2}$$

Where $\boldsymbol{J}$ is the columnwise stacked vector representing unknown two-dimensional current distribution; A is the matrix relating current distribution to the magnetic field distribution, calculated by FEM using the technique mentioned above, B is vector describing the magnetic field distribution. This equation was also described in Fig.2.
The inverse problem is then formulated as a linear least-squares problem:

$$\mathrm{Min}||A\boldsymbol{J}-B_m|| \tag{3}$$

Where B_m is the vector of the measured magnetic field values.
It is necessary to determine the current distribution (vector $\boldsymbol{J}$), which minimizes the quadratic residue between the calculated magnetic field and the measured field.
In order to determine the minimum number of magnetic sensors, at first the maximum sensors number was assessed, i.e. all possible probe placements were determined. The initial assessment showed that the sensors may be placed in two regions in the thruster – in the box fitted to the magnetic screen that was mentioned above and behind the anode, where the ratio of the Hall current self-field and primary magnetic field is also sufficiently high. Then the analysis was performed in order to exclude the sensors providing redundant information. More then 20 possible sensor locations were analyzed. The matrix of correlation coefficients corresponding to the matrix A was calculated. Several correlation coefficients are very close to 1, so the corresponding rows of the matrix A are almost linearly dependent, i.e. the corresponding sensors provide almost linearly dependent measurements. It means that one of each pair of sensors with high correlation coefficient value may be excluded. From each pair of the sensors with high correlation the sensor which location corresponds to the lower value of the Hall current self-field was excluded. The reason is that the higher the value of the magnetic field to be measured, the lower the expected measurements error.
The inverse problem was solved using the algorithm described below for different sensor combinations. After large amount of calculations the minimum number and optimal positions of the sensors were determined which give the most accurate results of the inverse problem solution. The chosen number of sensors is 5, which include two sensors behind the anode close to the channel centerline, one measuring radial and one axial magnetic field components and three sensors in the box inserted to outer magnetic screen – two for radial and one for axial magnetic field measurements.
So, we have obtained the linearized approximation of the inverse magnetostatic problem. The inverse magnetostatic problems are the particular case of the Fredholm integral equations of the first kind, which typically do not have a continuous inverse; therefore they are ill-posed[14]. The obtained problem is linear ill-posed problem; the problems of this type are essentially underdetermined. The standard methods of linear algebra such as LU, Cholesky or QR factorization cannot be used in a straightforward manner for their solution. It is necessary to incorporate some a priori information about the solution in order to stabilize the problem. This is the purpose of regularization. The key idea of the regularization is to approximate the discontinuous operator by a continuous one.
The condition numbers of matrices A_z and A_r corresponding to radial and axial magnetic field components in the entire longitudinal cross-section of the acceleration channel are 8.9759e+017 and 3.4274e+018. Obviously, these matrices are extremely ill-conditioned. Therefore, even if we know the magnetic field distribution in entire acceleration channel the straightforward solution of the inverse problem is impossible. The condition number of the matrix A corresponding to chosen sensors locations is 49.4 so the problem under consideration is also ill-conditioned. Since the number of equations (equal to the number of sensors) is less then the number of unknown values (equal to the number of current elements), the problem is also rank-deficient.

2. Regularization.

There are different regularization techniques applied to overcome the difficulties of solving discrete ill-posed problems. The most common form of regularization is Tikhonov regularization. In Tikhonov's method the ill-conditioning is circumvented by introduction of stabilizing term which gives the new problem with a well-

conditioned coefficient matrix. The Truncated Singular Value Decomposition (TSVD) method is based on replacing the small nonzero singular values from the decomposition of the operator by exact zeros giving the approximate well-conditioned operator. In iterative regularization the minimization problem (3) is solved using conjugate gradient method generating a family of continuous operators with the iteration number as a regularization parameter. Maximum entropy regularization which is used in image restoration and related applications uses the solution entropy as side constraint.

Different regularization methods were tested; the best results were obtained using the method based on Tikhonov regularization. The idea of the Tikhonov's method is to use a priori assumptions about the size and the smoothness of the desired solution. The general form of the Tikhonov's method for the problem (3) takes the form:

$$\min\left[\left\|A^* J - B_m\right\|^2 + \lambda^2 * \left\|LJ\right\|^2 \right] \tag{4}$$

Where λ is the regularization parameter which controls the weight of the regularization term relative to residual term, and L is the so-called discrete smoothing form - a matrix which defines the norm of the solution through which the "size" is measured. Typically L is the identity matrix, a diagonal weighting matrix or a discrete approximation of a derivative operator. The choice of the matrix L depends on the a priori properties of the solution, i.e. the additional information which is enforced on the regularization solution.

Different forms of the matrix L were tested including the identity matrix, corresponding to minimum-norm solution and different forms of two-dimensional derivative operators corresponding to the continuous and smooth solutions. From the physical considerations the current distribution should be smooth, and finally the following regularizing term was chosen:

$$L = \left\|L_{rr} J\right\|^2 + \left\|L_{zz} J\right\|^2 + 2\left\|L_{rz} J\right\|^2 \tag{5}$$

Where $L_{rr} = \frac{\partial^2 J}{\partial r^2}$, $L_{zz} = \frac{\partial^2 J}{\partial z^2}$ and $L_{rz} = \frac{\partial^2 J}{\partial r \partial z}$.

Additional constraints were added to the solution based on the physical features of the Hall current. The constraints used are:

1. Nonnegativity constraint. The physical meaning of this constraint is that azimuthal current in the entire acceleration channel flows in the same azimuthal direction. Without this constraint as is shown further, the obtained solution includes some elements with negative currents
2. Zero boundary condition. The azimuthal current on the walls of the acceleration channel is zero, the boundaries of the current distribution in the axial direction are always may be positioned so that the current density on them will be negligible.

The second constraint is added because the solution of the inverse problem with inexact data often contain secondary peaks on the boundary of the solution region which grow as the measurements error grows. Let us consider its physical meaning. The Hall current density is proportional to the axial component of the electric field and electron number density:

$$J = -ne\frac{E_z}{B_r} \tag{6}$$

Electron number density is equal to the ions number density. In the near-anode region both ions number density and axial electric field are very low, therefore the Hall current is close to zero. Outside the acceleration channel the electric field drops to zero and the Hall current also drops to zero at certain distance from the thruster exit plane. The zero value of the Hall current on dielectric walls is obvious.

To solve the problem (4), constrained optimization method described below was used.

The solution procedure is following – the simulated measurements are obtained using linear system (2), then the noise with maximum value of 10% is added. The initial values of current are set to zeros and the problem (4) is solved using the optimization method described below.
The regularized problem includes three derivatives and additional constraints, which make it different from traditional Tikhonov regularization. For that reason it proved impossible to use the usual methods such as L-curve for the regularization parameter choice. The parameter was chosen manually by the method described below.

3. Optimization method

The constrained minimization algorithm implemented in Matlab was used to solve (4). It is a Sequential Quadratic Programming algorithm which implementation consists of three main stages:

1. Updating of the Hessian of the Lagrangian function
2. Quadratic programming problem solution
3. Line search.

4. Results of inverse problem solution

For the numerical solution of the inverse problem the Matlab program has been developed. Using the methods described above the inverse problem is solved using exact or perturbed values of the magnetic field. As will be shown below, even the solution of the inverse problem using the exact values of the magnetic field is non-trivial taking into account the low number of sensors.

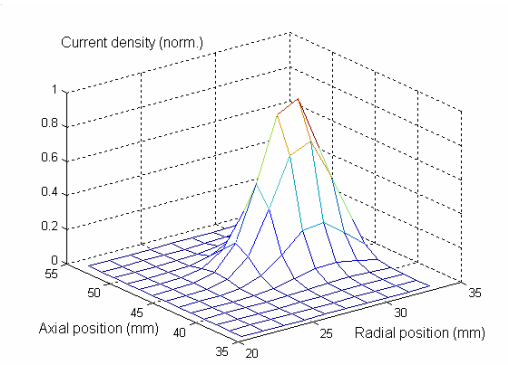

Figure 6. The Hall current distribution used for simulated measurements and inverse problem solution.
Position of the maximum: z=46 mm, r=30mm, total Hall current - 10A.

Let's consider the current distribution presented in Fig. 6. The peak of the distribution is situated several millimeters upstream of the exit plane close to the outer channel wall. This distribution is similar to the experimentally measured distribution of the Hall current density[4]. The simulated magnetic field values corresponding to magnetic sensors which positions were chosen according to the method described above are -12.0, -11.2, -43, -7.0 and 6.4 mG.
Solving the minimization problem without the constraints and regularization term will give the result shown in Fig. 7. Obviously, the solution is far from the exact distribution, besides it has no physical sense since the current density in some locations is negative, i.e. the currents in different elements flow in different azimuthal directions. Adding the non-negativity constraint we will obtain the solution shown in Fig. 8. This solution is also very far from the current distribution on Fig. 6. Obviously, it also lacks physical sense and cannot appear in acceleration channel. Adding the regularization term described above in order to obtain the smooth distribution will give the result presented in Fig. 9. This result is still very far from the original distribution. However, this distribution is continuous and smooth. This is the result of regularization term addition. Now adding the zero constraint at the borders of the solution domain we obtain the solution shown in Fig.10.
This solution is sufficiently close to the exact current distribution. The position of its peak coincides with the corresponding position of exact distribution; radial and axial widths of distribution are very close to those of the original distribution. The total current corresponding to this distribution is 10.6 which is close to the original value of 10 A. The relative error value is 6%. The radially averaged axial profiles as well as the axially averaged radial profiles corresponding to the original and calculated from "measurements distributions are presented in Fig 11. It should be emphasized that our objective is to obtain as much information as possible about the Hall current distribution but it is obviously impossible to obtain the exact distribution using such a low number of sensors. The obtained solution is close to the original distribution and the obtained accuracy is sufficient.

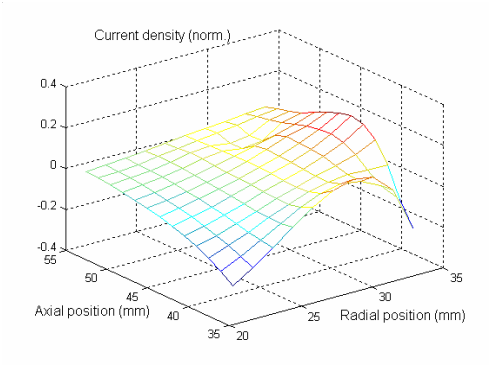

Figure 7. Solution of the inverse problem without regularization and constraints

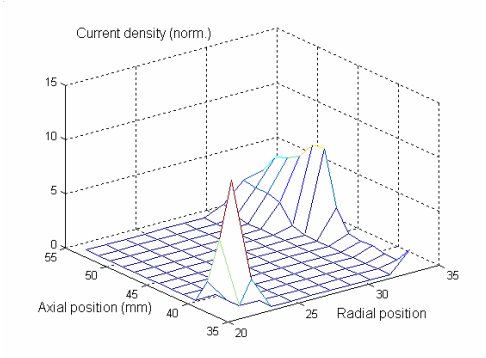

Figure 8. Solution of inverse problem with non-negativity constraint

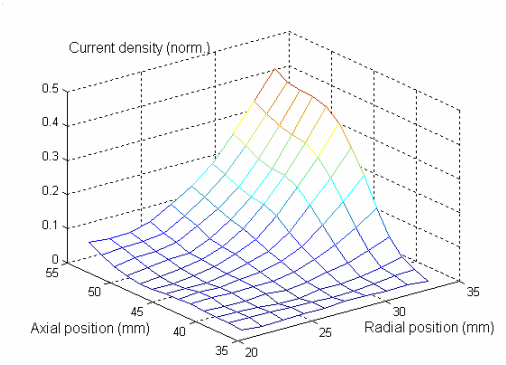

Fig. 9. Solution of the inverse problem with regularization term

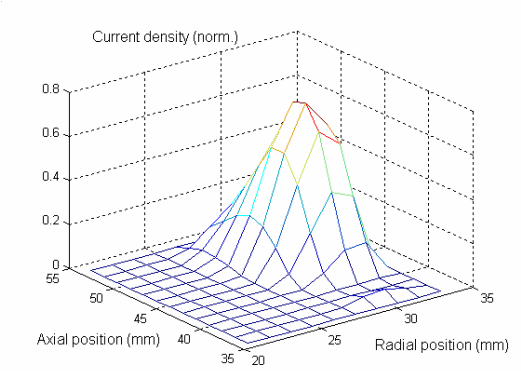

Fig. 10. The regularized solution with unperturbed measurements.

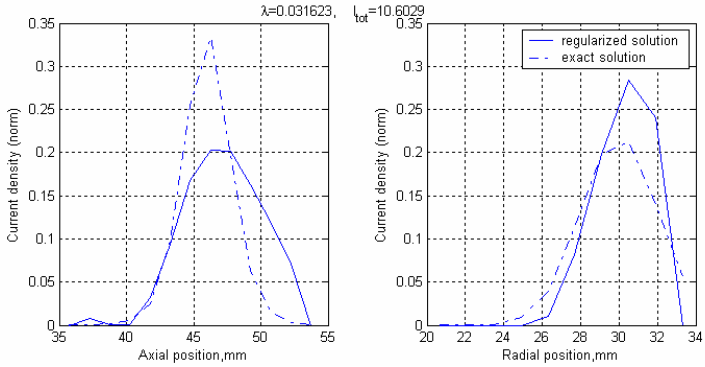

Fig. 11. Axial and radial profiles of original and calculated distributions.

The important step of solution is the choice of the regularization parameter. This parameter accounts for the degree of smoothness of the regularized solution. The most commonly used method for the regularization parameter choice is the L-curve method[14]. L-curve is the parametric plot of the discrete smoothing norm, i.e. the norm of the regularizing term $||LJ_{reg}||_2$ versus the corresponding residual norm $||A^*J_{reg} - B_m||_2$. For many discrete ill-posed problems this curve plotted in log-log scale has a characteristic L-shape with a distinct corner separating its horizontal and vertical parts. According to the L-curve criterion the value of the regularization parameter corresponding to the L-curve corner is the optimal value. In our case the curve does not have the L-shape and the optimal value of the regularization parameter marked with an arrow doesn't correspond to its distinct corner. The reason is that in this case the residual norm and the smoothing norm are not monotonic functions of the

regularization parameter. Another popular method for choosing the regularization parameter is the discrepancy principle. It requires the knowledge or a good estimate of the error norm. It is not possible to use it since the error norm is not known.

When it is not possible to use the parameter-choice methods the regularization parameter may be also chosen by visual inspection of the solution[15,16]. Since the parameter does not vary in wide range (10^{-3}-10^{0}) it is not very time-consuming.

The parameter choice procedure is demonstrated below. The set of solutions is obtained for different regularization parameter values and the minimal value corresponding to relatively smooth solution with a single peak is chosen. In the solution presented above 20 parameter values in the range from (10^{-3} to 10^{0}) uniformly spaced on the logarithmic scale were used. The corresponding solutions are presented on Fig. 12. Corresponding regularization parameter values and total current values are presented on the plots.

The solutions with low regularization parameter value are not smooth, have several sharp peaks and obviously may not be chosen. As the regularization parameter value increases, the solutions become smoother and the last two solutions are sufficiently smooth and have one distinct peak. The solution corresponding to the regularization parameter value 0.031623 is finally chosen. The comparison of the solution with the original distribution was presented above.

This results described above were obtained using the noise-free values of the simulated magnetic field measurements. The solution for the measurements perturbed with the 5% noise is presented in Fig. 13. Plots correspond to the same original measurements; the exact solution is given for comparison (dash-dot line). Because of the noise in the measurements the position of the maximum and the width of the distribution have slightly changed, but the obtained regularized solutions are still reasonable approximations to the exact solution. The radial position of the distribution center of mass is exact, the error in the axial position of center of mass is 2 mm and the error in the total current determination does not exceed 20 %.

The result shown on Fig.14 was obtained with 10% noise added to the measurements. In Fig. 15 some solutions corresponding to different current distributions with noise-free data and with noise added to the measurements. The total current of the original distribution is 10 A in all cases. The error in the peak position does not exceed 2 mm and the error in total current does not exceed 25%.

As may be seen, for the different distributions of the Hall current the main figures of merit – position of the peak and total current value are determined with sufficient accuracy, both with noise-free and with the perturbed data. In most cases the width of the distribution is also a reasonable estimation of the original width but in some cases the narrow axial distribution is over-smoothed. Obviously, as the measurement error norm increases, the accuracy of the inverse problem solution decreases.

There is a trade-off between the number of sensors and the accuracy of the inverse solution. For example, for two cases corresponding to the same original distribution but with different number of sensors, 4 and 5 accordingly with 10% noise added in both cases, the position and the width of the peak are almost the same for both regularized solutions, however, the error in the total current is 35 % in the case of 4 sensors and 24% in the case of 5 sensors. Therefore, the number of the sensors may be chosen according to the necessary accuracy level.

III. Conclusion

1. The method of Hall current structure determination proposed in Ref. 3 is further developed. It is shown that the Hall current structure can be determined using non-contact steady-state measurements of magnetic field.
2. Three-dimensional analysis of the magnetic fields in Hall thruster was carried out in order to determine the optimal magnetic sensors positions. Optimal number of sensors was also determined.
3. Solution of inverse magnetostatic problem was obtained for the determination of Hall current structure from magnetic measurements. Two-dimensional axysimmetric Hall current distribution was used in calculations. The algorithm of inverse problem solution is based on two-dimensional constrained regularization.
4. Solution algorithm was tested using both noiseless and noisy simulated magnetic measurements. The solution with simulated measurement noise up to 10% of primary signal gives reasonable result.

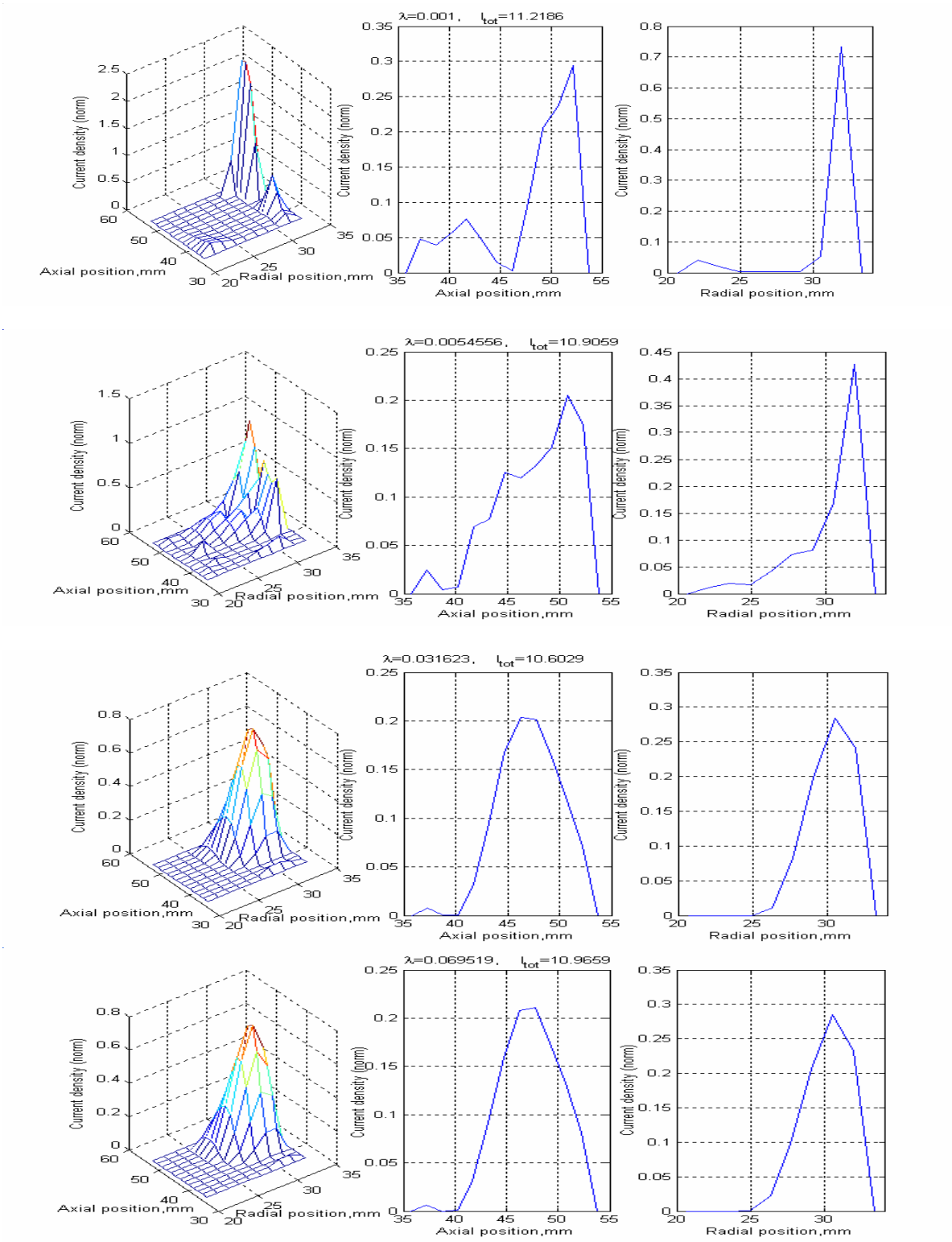

Fig. 12. Solutions corresponding to different values of regularization parameter

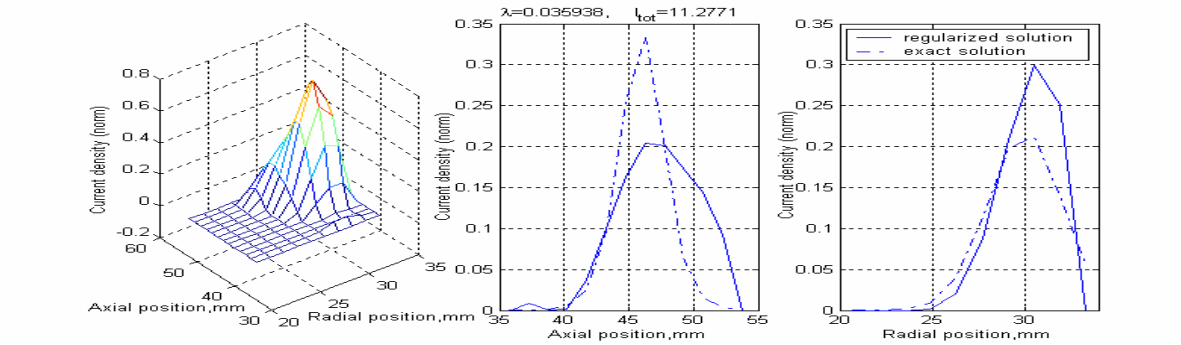

Fig. 13. Inverse problem solution corresponding to measurements with 5% noise added

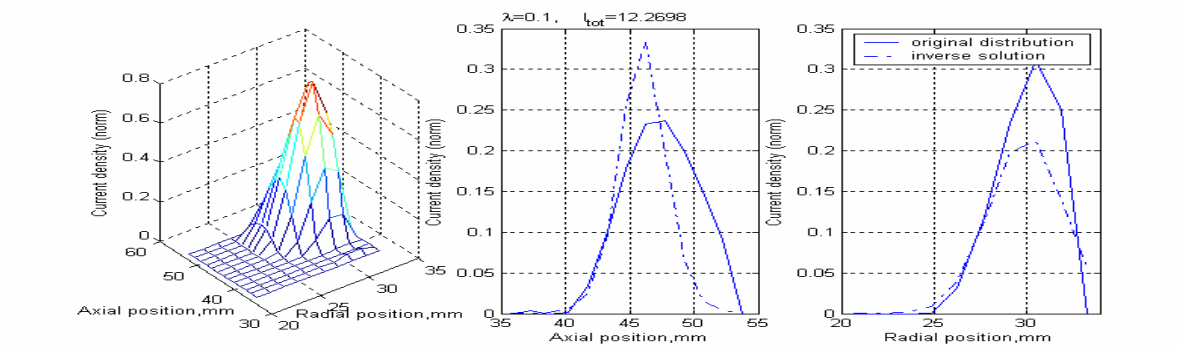

Fig. 14. Inverse problem solution corresponding to measurements with 10 % noise added

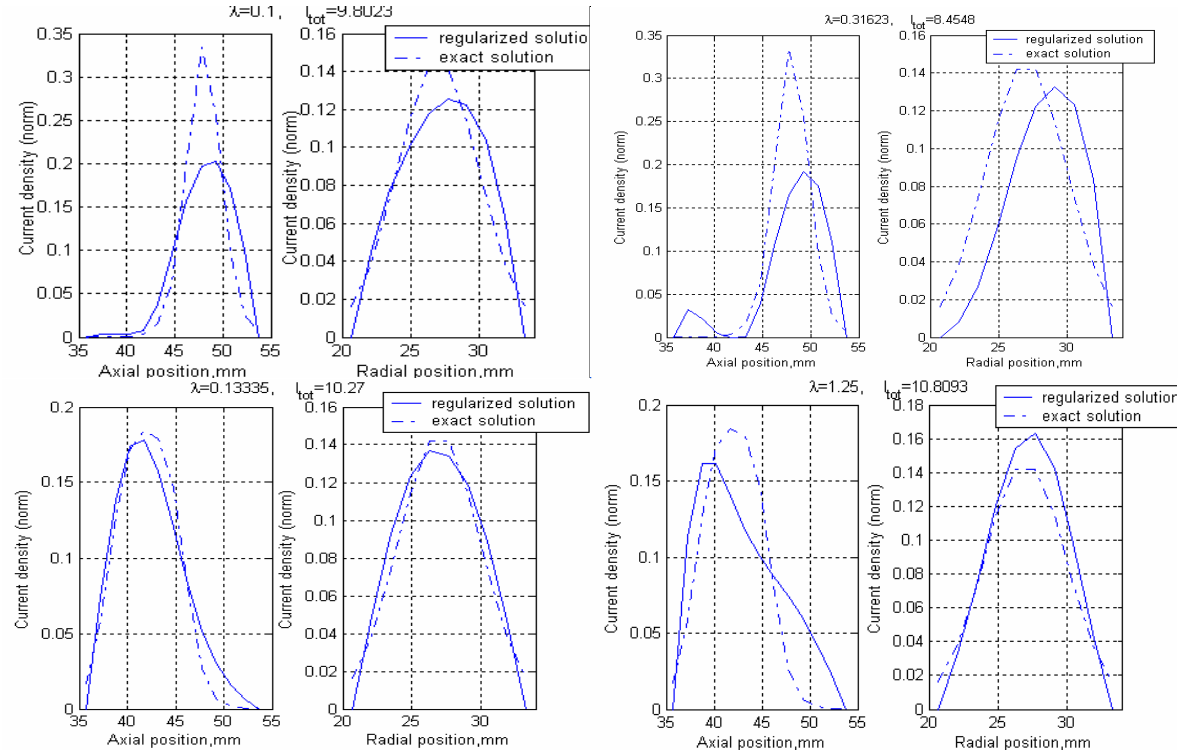

Fig. 15 Inverse problem solutions with noise-free data (left) and 10% noise added (right) for different original distributions.

References

[1]Manzella, D., Jankovsky, R., Elliott, F., et al.., "Hall Thruster Plume Measurements On-board the Russian Express Satellites." IEPC Paper 2001-044, 27-*th International Electric Propulsion Conference,* 2001.

[2]Kapulkin, A., Kogan, A., Guelman, M., "Noncontact Emergency Diagnostics of Stationary Plasma Thruster in Flight," *Acta Astronautica,* Vol. 55 (2004), pp.109-119.

[3]Rubin, B., Guelman, M., Kapulkin, A., "Principles of Hall Thruster Onboard Malfunction diagnostics Based on Magnetic Field Measurements of Plasma Currents", *4th International Symposium on Spacecraft Propulsion*, 2004.

[4]Haas, J.M., Gallimore, A.D., "Considerations on the Role of the Hall Current in a Laboratory-Model Thruster," AIAA Paper 2001-3507, *37-th Joint Propulsion Conference,* 2001.

[5] Demyanenko, V.N., Zubkov, I.P., Lebedev, S.V., Morozov, A.A., "Induction Method for Measuring the Azimuthal Drift Current in a Hall-Current Accelerator", *Soviet Phys. Tech. Phys.* Vol.23, No. 3, March 1978, pp.376,377 .

[6] Bugrova, A.I., Versotskii, V.S., Kharchevnikov, V.K., "Determination of the Radial Center of Gravity of an Azimuthal Drift Current in Accelerators with Closed Electron Drift", *Soviet Phys. Tech. Phys.,* Vol. 25, No.10, October 1980, pp.1307-1309.

[7] Prioul, M., Bouchoule, A., Roche, S., Magne, L., Pagnon, D., et al.., "Insights of Hall Thrusters through Fast Current Interruptions and Discharge Transients", IEPC Paper 01-059, 27-*th International Electric Propulsion Conference,* 2001.

[8]Thomas, C.A., Gascon, N., Cappelli, M.A., "Non-Intrusive Characterization of the Hall Thruster Azimuthal Drift Current", AIAA Paper 2004-3776, *40-th Joint Propulsion Conference,* 2004.

[9]Begot, S., Voisin, E., Hiebel, P., Kauffmann, J.M., Artioukhine, E.A., "Resolution of Linear Magnetostatic Inverse Problem Using Iterative Regularization", *The European Physical Journal AP*, Vol. 12, No.11, November 2000, pp.123-131.

[10] Nenonen, J.T., "Solving the Inverse Problem in Magnetocardiography", *IEEE Engineering in Medicine and Biology*, Vol. 13, 1994, pp. 487-496.

[11] Bettini, P., Bellina, F., Formisano, A., Martone, R., et al., "Identification of the Plasma Magnetic Contour from External Magnetic Measurements by Means of Equivalent Currents", *The European Physical Journal AP*, Vol. 13, No.1, January 2001, pp. 51-58.

[12]Chadebec, O. Coulomb, J.-L., Bongiraud, J.-P., Cauffet, G., Le Thiec, P., "Recent Improvements for Solving Inverse Magnetostatic Problem Applied to Thin Shells", *IEEE Transactions on Magnetics*, Vol. 38, No. 2, March 2002, pp. 1005-1008.

[13]Russenschuk, S., Calmon, F., Lewin, M., Ramberger, S., et al., "Integrated Design of Superconducting Accelerator Magnets. A Case Study of the Main Quadrupole", *The European Physical Journal AP*, Vol. 1, No.1, January 1998, pp.93-102.

[14]Per Christian Hansen, *Rank-Deficient and Discrete Ill-Posed Problems: Numerical Apsects of Linear Inversion*, SIAM Monographs on Mathematical Modeling and Computation 4, SIAM, Philadelphia, 1997.

[15]Merwa, R., Hollaus, K., Brunner, P., Scharfetter, K., "Solution of the Inverse Problem of Magnetic Induction Tomography (MIT)", *Physiological Measurement, Vol.* 26, March 2005, pp. 241-250

[16]Casanova, R, Silva, A., Borges, A.R., "Magnetic Induction Tomography Imaging Using Tikhonov Regularization", *Workshop on Inverse Obstacle Problems,* Lisbon, 2002.